Minocycline suppresses disease-associated microglia (DAM) in a model of photoreceptor cell degeneration

Sarah Doyle (sarah.doyle@tcd.ie)
Trinity College Dublin https://orcid.org/0000-0002-6294-9380
Ema Ozaki
Trinity College Dublin: The University of Dublin Trinity College
Conor Delaney
Trinity College Dublin: The University of Dublin Trinity College
Matthew Campbell
Trinity College Dublin: The University of Dublin Trinity College

Research

Keywords: disease-associated microglia, minocycline, retinal degeneration, lipoprotein lipase

Posted Date: July 20th, 2021

DOI: https://doi.org/10.21203/rs.3.rs-656962/v1

Title: Minocycline suppresses disease-associated microglia (DAM) in a model of photoreceptor cell degeneration.

Authors: Ema Ozaki[1, 2], Conor Delaney[3], Matthew Campbell[3], Sarah L. Doyle[1,2,4]

Affiliations:

[1]Department of Clinical Medicine, School of Medicine, Trinity College Dublin, Dublin, Ireland.

[2]Trinity College Institute of Neuroscience, Trinity College Dublin, Dublin, Ireland.

[3]Smurfit Institute of Genetics, Trinity College Dublin, Dublin, Ireland.

[4]National Children's Research Centre, Our Lady's Children's Hospital Crumlin, Dublin, Ireland.

Corresponding Author:

Dr. Sarah Doyle, e-mail: sarah.doyle@tcd.ie tel: +353 1 8963011

Key words: disease-associated microglia, minocycline, retinal degeneration, lipoprotein lipase

Abstract:

Background: As the resident immune cells in the retina, microglia play important homeostatic roles in retinal immune regulation and neuroprotection. However, chronic microglia activation is a common hallmark of many degenerative retinal diseases. The semi-synthetic broad spectrum tetracycline antibiotic, minocycline appears to inhibit pro-inflammatory microglia which coincides with protection against photoreceptor cell degeneration. A sub-type of microglia termed disease associated microglia **(**DAM) have recently been associated with a wide range of central nervous system (CNS) diseases.

Methods: In this study we examine the kinetics of microglia infiltration towards the outer retina of rhodopsin knockout mice (*rho*$^{-/-}$) by immunofluorescence, and undertake transcriptional and spatial localization analysis of markers for evidence of both homeostatic function and appearance of DAMs.

Results: We demonstrate in the *Rho-/-*mice that Iba1^{+} and P2RY12^{+} microglia take on activated morphology early in disease, prior to notable photoreceptor loss and are capable of infiltrating the subretinal space. Expression of lipid processing enzyme and DAM-marker lipoprotein lipase (LPL) is primarily observed only after microglia have traversed the ONL. Administration of minocycline to *Rho-/-*mice induced loss of phagocytic/DAM microglia in the outer retina *in vivo* coinciding with photoreceptor survival and amelioration of retinal degeneration.

Conclusion: Our study identifies microglial lipid processing enzyme and DAM-marker LPL as a direct target of minocycline and indicates that suppression of lipid metabolism is one mechanism by which minocycline protects against inflammation induced photoreceptor cell death.

Introduction

Retinal degeneration is a progressive neurodegenerative condition and encompasses a cohort of inherited, acquired and age-related diseases that can lead to severe visual impairment and eventual blindness. Retinitis pigmentosa (RP) is a genetically heterogeneous category of inherited photoreceptor degenerations for which retinal gene therapies targeting X-linked RP with variants in the *RPGR* gene and *RPE65*-related Leber congenital amaurosis (LCA) are proving promising. However, while gene therapies may have benefit for those individuals with mutations in the targeted genes, no broad-spectrum effective treatments exist for this condition. Photoreceptor cells are specialised neurons that convert light into electrical signals that are deciphered in the brain. Identification of unifying processes that can protect photoreceptors from premature death has potential to offer a global therapeutic approach for prolonging sight across multiple inherited blinding diseases.

Retinal inflammation is thought to accelerate the pace of progression of photoreceptor cell death irrespective of the underlying cause of disease, and suppression of microglial activation has been shown to be neuroprotective in mouse models of retinal degeneration (Peng, Xiao et al. 2014, Murakami, Ishikawa et al. 2020). Recent advances in single-cell analysis have uncovered subtleties in microglia subtypes that are associated with a wide range of neurodegenerative diseases termed DAM (disease associated microglia) (Keren-Shaul, Spinrad et al. 2017). These DAM appear to be highly effective at phagocytosing debris and unwanted protein aggregates and may in fact be beneficial if triggered early in disease where strong phagocytic activity is desirable.

In this study, we examine the kinetics of microglia infiltration towards the outer retina of rhodopsin knockout mice (*Rho*$^{-/-}$), and undertake transcriptional and spatial localization analysis of markers for evidence of both homeostatic function and appearance of DAM. The *Rho-/-*retina develops normal numbers of rod and cone nuclei, but the rods have no outer segments and ensuing rod degeneration becomes evident histopathologically from 3 weeks (Ozaki, Gibbons et al. 2020). Rod photoreceptor degeneration is followed by cone photoreceptor degeneration with a complete loss of electrical responsiveness by 8 wk. At 12 wk, the majority of photoreceptors in the retina are lost (Humphries, Rancourt et al. 1997). In this study, we demonstrate in the *Rho-/-* mice that Iba1^{+} and P2RY12^{+} microglia take on activated morphology early in disease, prior to notable photoreceptor loss and are capable of infiltrating the subretinal space (SRS), an immune privileged site usually devoid of microglia. Prior to crossing through the photoreceptor outer nuclear layer (ONL) microglia express CD68 further indicating presence of an inflammatory environment. Interestingly expression of lipid processing enzyme and DAM-marker lipoprotein lipase (LPL) is primarily observed only after microglia have traversed the ONL. Recent literature indicates that the semi-synthetic broad spectrum tetracycline antibiotic, minocycline, may have potential to counter-regulate pro-inflammatory microglia and protect photoreceptor cell degeneration (Peng, Xiao et al. 2014, Scholz, Sobotka et al. 2015, Terauchi, Kohno et al. 2021). Administration of minocycline to *Rho-/-*mice reduced markers of DAM in the degenerating *Rho-/-*retina and prevented microglia infiltration into the SRS. Minocycline has many cell and molecular targets; here we show that it acts directly on microglial cells, significantly reducing DAM-markers APOE and LPL among others, *in vitro,* and furthermore, inhibits microglia phagocytic function. In turn, minocycline-induced loss of phagocytic/DAM microglia in the outer retina *in vivo* coincides with photoreceptor survival and amelioration of retinal

degeneration. Our study identifies microglial LPL as a direct target of minocycline and indicates that suppression of lipid metabolism is one mechanism by which minocycline protects against inflammation induced photoreceptor cell death.

Materials and Methods

Animals

All studies carried out in the Smurfit Institute of Genetics in TCD adhere to the principles laid out by the internal ethics committee at TCD, and all relevant national licenses were obtained before commencement of all studies. C57BL/6J mice were sourced from Jackson Laboratory and bred on-site at the Smurfit Institute of Genetics in TCD. *Rho-/-*mice were kindly provided by Prof Peter Humphries, TCD. Before experiments, all mice were kept on a 12-h light/dark cycle.

Minocycline administration

*Rho-/-*mice received intra-peritoneal injections of 50 mg/kg minocycline (Sigma-Aldrich) or vehicle H_2O twice daily, starting from postnatal day 16 and continuing till postnatal day 21 or 42.

Optical Coherence Tomography (OCT) analysis

OCT was performed on mice using a Heidelberg Spectralis OCT (Heidelberg Engineering). Pupils were dilated with 1 % tropicamide and 2.5 % phenylephrine and mice anaesthetized using a mixture of ketamine/medetomidine (100/0.25 mg/kg). OCT images were captured with a 30° angle of view. Heidelberg eye explorer version 1.7.1.0 was used to capture

images. ImageJ (National Institutes of Health, Rockville, MD, USA) was used for quantification analysis.

H&E staining

Mouse eyes were fixed in Davidson's Fixative for 24 h, followed by three PBS washes. Eyes were processed in a tissue processor under gentle agitation as follows: 70 % ethanol for 1 h, 80 % ethanol for 1 h, 95 % ethanol for 1 h, 100 % ethanol for 1 h, 100 % ethanol for 1 h, 50 % ethanol/xylene mix for 1 h, xylene for 1 h, xylene for 1 h, paraffin at 60°C for 1 h, and paraffin under vacuum at 60 °C for 1 h. Eyes were then embedded in paraffin and 5 µm sections were collected onto Polysine slides using a microtome. The sections were deparaffinized by dipping ten times in xylene, followed by rehydration in 10 dips each of 100 %, 90 %, and 70 % ethanol. The slides were incubated in haemotoxylin solution for 6 min, rinsed in water, and then incubated in eosin solution for 2 min. The slides were rinsed in water and dehydrated by dipping ten times in 70 %, 90 %, and 100 % ethanol and once in xylene. The slides were mounted using the Sub-X Mounting Medium and analyzed under a light microscope (Olympus 1X81).

Immunohistochemistry

For retinal cryosections, mouse eyes were fixed in 4 % paraformaldehyde for 1 h and 30 min at room temperature, followed by three PBS washes. Eyes were cryoprotected in 20 % sucrose for 1 h, followed by 30 % sucrose overnight at 4 °C, and subsequently embedded and frozen in an optimum cutting temperature compound. 12-µm sections were collected onto Polysine slides using a cryostat. Cryosections were block and permeabilized with 5% NGS and 0.05% Triton in PBS for 1 h at room temperature. The slides were incubated overnight at 4°C in a humidity

chamber with primary antibody diluted in 5 % NGS. Primary antibodies used were Iba1 (Wako, 019-19741, 1:500), CD68 (Abcam, ab53444, 1:200), P2RY12 (AnaSpec ANA55043A, 1:100), and LPL (Abcam, ab21356, 1:100). After three PBS washes, the cryosections were incubated with Alexa Fluor 594- and 488-conjugated goat anti-rabbit, Alexa Fluor 488-conjugated anti-mouse and Alexa Fluor 594-conjugated anti-rat secondary antibodies (1:500; Invitrogen) diluted in 5% NGS for 2 h at room temperature and counterstained with Hoechst 33342 (1:10,000). The slides were mounted with Hydromount (VWR) mounting medium and analyzed using a confocal microscope (Zeiss LSM 710).

For retinal flat-mounts, mouse eyes were fixed in 4 % paraformaldehyde for 15 min. After a PBS wash, the cornea and lens were carefully removed, and four incisions were made into the retinal eye cup to flatten out the tissue. Retinal flatmounts were fixed for a further 15 min in 4% paraformaldehyde. After three PBS washes, flat-mounts were permeabilized and blocked overnight in 10 % NGS and 1 % Triton in PBS at 4° C. Flatmounts were incubated with Iba1 antibody for 48 h at 4°C in a humidity chamber. After three PBS washes flat-mounts were incubated with Alexa Fluor 594-conjugated anti-rabbit secondary antibody for 24 h at 4 °C. Flat-mounts were mounted with Hydromount (VWR) mounting medium and analyzed using a confocal microscope (Zeiss LSM 710) and ImageJ software. All image analysis was performed using ImageJ.

Cell culture

The mouse microglial BV2 cell line was cultured in RPMI with 10% FBS, supplemented with 10 % fetal calf serum (Sigma-Aldrich) and 1 % penicillin/streptomycin (Sigma-Aldrich) and

maintained at 37 °C in a humidified 5 % CO_2 atmosphere. The cells were seeded at 5×10^4 cells per cm^2 and incubated overnight before treatment. BV2 cells were treated 5 mg/ml minocycline or sterile H_2O as vehicle control. Cells were harvested 6 h and 24 h after treatment.

Phagocytosis Assay

BV2 cells were plated on chamber slides and treated with 5 ug/ml minocycline for 21 h prior to being assayed. Polystyrene amine modified (yellow-green) latex beads (Sigma-Aldrich) were pre-opsonised in FBS (1:5) at 37 °C for 1h. Opsonized beads were diluted 1:2,000 in media and added to cells for 3 h. Cells were washed with ice-cold PBS 3 times to remove surface bound beads, fixed in 4 % PFA for 10 min and stained with MitoTracker Orange CMTMRos for 30 min. Cells were washed and counterstained with Hoechst 33342 (1:10,000). Cells were imaged on a BX51 Olympus microscope and analyzed by ImageJ.

qRT-PCR analysis

Total RNA was extracted from BV2 cells or mouse retinas using Isolate II RNA extraction kit (Bioline) as per the manufacturer's instructions. RNA was reverse transcribed using MMLV Reverse Transcriptase (Promega). Target genes were amplified by real-time PCR with SensiFast SYBR Green (Bioline) using the ABI 7900HT system (Applied Biosystems). The comparative CT method was used for relative quantification after normalisation to the "housekeeping" gene ubiquitin C (UBC). Primers used were as follows:

Target	Forward Primer (5’-3’)	Reverse Primer (5’-3’)
APOE	ATTGCTGACAGGATGCCTAGC	GGTTGGTTGCTTTGCCACTC
AXL	TTCAACTGTGCTACGTCCCC	GGGTCCCTCTAGGTAAGCCA
CLEC7a	GTGGTAGTAGTGGTTGCTGC	ATTCTGTGGGCTTGTGGTTC
CSF1R	AAGCAGAAGCCGAAGTACCA	GTCCCTGCGCACATATTTCAT
CTSB	CAGGCTGGACGCAACTTCTA	GCCCCAAATGCCCAACAAG
CX3CR1	CTGTTATTTGGGCGACATTG	AACAGATTTCCCACCAGACC
iNOS	ATGGACCAGTATAAGGCAAGC	GCTCTGGATGAGCCTATATTG
ITGAX	CGATGCCTTCCCATGAATACG	CTTGGTGTCTCTGTGCCCTC
LGALS3	CTCTGACAGCTAGCGGAGC	AGGCATCGTTAAGCGAAAAGC
LPL	TCGTCATCGAGAGGATCCGA	TGTTTGTCCAGTGTCAGCCA
P2RY12	CAAGGGGTGGCATCTACCTG	AGGCAGCCTTGAGTGTTTCTG
SALL1	TTTCCAATCCGACCCCGAAG	CCACAGACATGGGCATCCTT
SELPLG	GGGATGGTCCTTCCTTTGGG	ACAATGGTCTAAGCGCCCTC
SPP1	CTGGCTGAATTCTGAGGGACT	CTGCTTCTGAGATGGGTCAGG
TGFBR1	AGCTCCTCATCGTGTTGGTG	GGCCTGTCTCGAGGAATTAGG
TMEM119	TTCACCCAGAGCTGGTTCCATA	TCTCCGGTGTGGGACTGAA
TREM2	ACAGCACCTCCAGGAATCAAG	AGGATCTGAAGTTGGTGCCC
TYROBP	GGTGTACTGGCTGGGATTGT	GCAATGTGTTGTTTCCGGGT
UBC	CCCAGTGTTACCACCAAGAAG	CCCCATCACACCCAAGAACA

183

184

185

Western blot analysis

Retinal tissue and BV2 cells were lysed in RIPA lysis buffer with phosphatase and protease inhibitors (Sigma-Aldrich) and centrifuged at 15,000 *g* for 15 min. Protein lysates were resolved on 10 % or 12 % SDS polyacrylamide gels and transferred to a PVDF membrane. Membranes were blocked in 5 % non-fat milk in Tris-buffered saline containing 0.05% Tween-20 (TBST) for 1 h and then incubated overnight at 4 °C in primary antibodies against APOE (Merck, 178479, 1:2000), LPL (Abcam, ab21356, 1:1000), Galectin-3 (R&D, AF1197, 1:2000), CSF1R (Invitrogen, PA5-25974, 1:500) and β-actin (1:2,000; Sigma-Aldrich). After three TBST washes, the membranes were incubated in horseradish peroxidase–conjugated anti-rabbit, anti-mouse or anti-goat antibodies (1:2,000; Sigma-Aldrich) for 1 h at room temperature. After three TBST washes, the membranes were developed using enhanced chemiluminescence (Advansta). Densitometry was performed using ImageJ, with SARM1 levels normalized to the loading control β-actin.

Results

Microglia are activated and infiltrate the outer retina in the rhodopsin knockout model of photoreceptor degeneration

Microglia are morphologically and functionally dynamic cells that can transform from a highly ramified state into a rod or amoeboid state during activation and pathology. Under basal or physiological conditions, ramified microglia predominate. However, in response to injury or inflammatory conditions, de-ramification occurs where microglial processes shorten and thicken and cell bodies expand, ultimately shifting into a round amoeboid shape (Karperien, Ahammer et al. 2013). Here, we examine microglia dynamics in the *Rho-/-*model of retinal degeneration. *Rho-/-*mice develop a normal number of rod and cone nuclei but with the absence of rod outer segments (OS), these cells begin to degenerate from 3 weeks of age and by 12 weeks most of the photoreceptors are lost. To visualize and characterize the role of microglia in the *Rho-/-*model of retinal degeneration we performed immunofluorescence on retinal flatmounts of the microglia marker Iba1 in wild-type and Rho-/-mice at 3, 6, 9 and 12 weeks of age (**Fig. 1A**). At all time-points observed, wild-type microglia had a ramified appearance with long fine processes and small cell bodies indicative of physiological 'surveillant' microglia (**Fig. 1A, first column**). In the contrary, microglia in the *Rho-/-*retinal flatmounts had an activated appearance with larger cell bodies and retracted processes (**Figure 1A, second column**), which are particularly evident in the high magnification and skeleton images (**Fig. 1A, a'-h'**). De-ramified microglia were evident from as early as 3 weeks of age (**Fig. 1A, a', b'**), demonstrating that microglial activation occurs from a very early age in the *Rho-/-*mice. To examine the distribution of

microglia within the laminar structure of the retina in the *Rho-/-*mice, we stained cross sections of the retina from these mice at 3, 6, 9 and 12 weeks of age with Iba1. In the wild-type retina, Iba1-stained microglia were observed in the synaptic inner plexiform (IPL) and outer plexiform layers (OPL) (**Fig. 1B, first column**). However, in the retinal cryosections from *Rho-/-*mice, Iba1-stained microglia were seen to migrate into the outer nuclear layer (ONL) and down towards the photoreceptor inner and outer segments or sub-retinal space (SRS) (**Figure 1B, second column**).

Microglia infiltrating the SRS are actively phagocytosing photoreceptor cells and express disease associated microglia (DAM) marker LPL

Next, we sought to analyse the microglia infiltrating the SRS for markers of phagocytosis and markers of homeostatic function. First, we stained retinal cryosections from 12 week old wild-type mice **(Fig. 2A, top row)** and *Rho-/-*mice at 3, 6, 9 and 12 weeks of age with CD68, a lysosomal protein that is upregulated in actively phagocytic cells. In wild-type sections, no co-localization of CD68 and Iba1 were observed, and fluorescence was mainly seen in the OPL likely due to non-specific IgG staining in the blood vessels **(Fig. 2A, top row)**. CD68 positive staining was significantly increased in Rho-/-cryosections and co-localization of Iba1 and CD68 was observed in microglia in the OPL and in microglia that had infiltrated the ONL and SRS **(Fig.s 2A a' & 2A b')**. As Iba1 is also expressed in macrophages, we next stained retinal cryosections with the more recently identified microglial-specific homeostatic marker P2RY12 (**Fig. 2B**). Although some studies have found a decrease in microglial homeostatic genes like P2RY12 in aging and neurodegenerative models, we found P2RY12 immunopositivity in both wild-type cryosections (**Fig. 2B**, **top row**) and *Rho-/-*cryosections at 3, 6, 9 and 12 weeks of age

(**Fig. 2B**, **rows 2-5**). Co-staining with CD68 also revealed co-localization of CD68 and P2RY12 in the activated microglia in the OPL, ONL and SRS of *Rho-/-*mice **(Fig.s 2B a' and 2B b')**. Finally, retinal cryosections from wild-type and *Rho-/-*mice were stained with lipoprotein lipase (LPL) **(Fig. 3)**. LPL, an enzyme that hydrolyses triglyceride rich lipoproteins, is associated with an alternatively activated and highly phagocytic microglial phenotype. In wild-type retinas, no LPL reactivity was observed in microglia with fluorescence only observed in blood (either due to non-specific IgG staining or specific staining of vessel walls) **(Fig. 3A)**. In contrast, LPL immunopositivity was observed in *Rho-/-*retinas at 3, 6, 9 and 12 weeks of age and co-staining with Iba1 revealed co-localisation with microglia that resided solely in the SRS; Iba1-positive microglia in the inner retina remained LPL-negative **(Fig.s 3A a' b' c' & d', white arrows)**.

Minocycline downregulates DAM genes in the rhodopsin knockout model of retinal degeneration

Minocycline, a broad-spectrum tetracycline antibiotic, has previously been reported to ameliorate photoreceptor cell death in numerous mouse models of retinal degeneration (Zhang, Lei et al. 2004, Kohno, Chen et al. 2013, Peng, Xiao et al. 2014, Scholz, Sobotka et al. 2015, Dannhausen, Möhle et al. 2018, Terauchi, Kohno et al. 2021) and is a known inhibitor of microglial activation. Given the interesting LPL staining pattern we had observed in the *Rho-/-*retina, we wanted to examine the effects of minocycline on genes associated with homeostatic function and those that are a signature of disease-associated microglia (DAM). DAM-related genes of which LPL is a key member have been revealed due to recent advances in single cell technologies. We injected *Rho-/-*mice with 50 mg/kg of minocycline or vehicle (H_2O) control twice a day from post-natal day 16 (P16) until the mice were sacrificed at 3 weeks of age. Immunofluorescence of Iba1 in

retinal flatmounts from these mice showed a significant reduction in activated microglia with minocycline treatment, with the cells having a more ramified morphology compared to vehicle injected mice **(Fig. 4A)**. The difference in morphology was confirmed using the grid cross method where the ramified microglia from minocycline injected animals had greater numbers of grid cross points compared to the shorter cellular processes of the vehicle injected *Rho-/-*mice **(Fig. 4B)**. We then assessed the neural retina of minocycline or vehicle injected *Rho-/-*mice for signature markers of homeostatic microglia and DAM. Out of the 6 homeostatic microglial genes (*Cx3cr1, P2ry12, Sall1, Tgfbr1, Selplg, Tmem119*) assessed by quantitative real-time PCR, expression levels of 5 remained unchanged while *Sall1* was found to be downregulated in retinas from minocycline injected mice **(Fig. 4C**). Interestingly, the DAM signature genes (*Apoe, Axl, Clec7a, Ctsb, Csf1r, Itgax, Lgals3, Lpl, Spp1, Trem2, Tyrobp*) were found to be more transcriptionally dynamic with a reduction in *Apoe*, *Axl*, *Clec7a*, *Csf1r*, *Ctsb* and *Lpl* levels in retinas from minocycline injected mice while *Itgax* levels increased **(Fig. 4C)**. The gene expression profiles of these microglial genes are illustrated in a heatmap **(Fig. 4D)** and also shows the levels of expression of these genes in the retina with genes most highly expressed in the retina in red and those least expressed in blue. As one of the most significantly DAM genes downregulated by minocycline at the transcriptional level, LPL levels were further examined in retinal cryosections from these mice. In vehicle-injected 3-week-old *Rho-/-*mice, LPL and Iba1 co-localization was observed in microglia residing in the SRS whereas LPL was absent in all microglia in minocycline injected animals **(Fig. 4E)**.

Minocycline directly regulates DAM gene expression in BV2 microglia in vitro.

As the neural retina is composed of many different cell types, we next sought to examine how minocycline affects homeostatic and DAM gene expression profiles specifically in microglia, using the BV2 mouse microglia cell line. Minocycline is known to inhibit M1 polarization in microglia, (Kobayashi, Imagama et al. 2013) so we first confirmed by quantitative real-time PCR analysis that transcriptional levels of the M1 marker iNOS was significantly reduced in BV2 cells after minocycline (5 ug/ml) treatment (**Fig.5A 1st panel)**. Interestingly, we saw no significant changes in the 6 homeostatic microglial genes (*Cx3cr1, P2ry12, Sall1, Tgfbr1, Selplg, Tmem119*) assessed while minocycline significantly reduced 3 of the DAM genes, *Clec7a*, *Lpl* and *Tyrobp* **(Fig. 5A)**. Again, the gene expression profiles of these microglial genes are illustrated in a heatmap **(Fig. 5B)** with the most highly expressed genes in red and the least expressed in blue. Next, we investigated whether minocycline could alter the protein expression levels of some of these microglial markers by Western blot analysis. Similar to what was observed at the transcriptional level, minocycline significantly reduced LPL protein expression (**Fig. 5C**). As LPL is a key enzyme involved in lipid metabolism, we also examined levels of apolipoprotein E (ApoE), a lipid and cholesterol transporter that is prominently associated with neurodegenerative disease. Although we did not see any changes in *Apoe* at the transcriptional level in BV2 cells, minocycline significantly reduced both 34-kDa full-length ApoE protein as well as ApoE fragments observed at 28- and 22-kDa (**Fig. 5D**). CSF1R (colony stimulating factor 1) levels were also significantly decreased by minocycline (**Fig. 5E)**, despite not being altered at the transcriptional level. CSF1R is a primary regulator of microglial, proliferation, migration, differentiation and survival and has been found to be upregulated in inflammatory and neurodegenerative disease. Finally, we looked at protein levels of the DAM marker Galectin-3.

Lgasl3, the gene encoding galectin-3, was significantly upregulated in the minocycline injected *Rho-/-*retinas, however, protein levels remained unchanged in minocycline treated BV2 cells **(Fig. 5F)**.

Minocycline inhibits microglial phagocytic function and supports photoreceptor survival in the *Rho-/-*retinal degeneration model.

It was clear that minocycline reduced LPL-positive microglia in the SRS of the *Rho-/-*retina (**Fig. 4E).** We sought to further examine the effect of minocycline influence on microglia migration. Retinal cryosections from *Rho-/-*mice that had received two daily injections of minocycline or vehicle control from P16 to P21 or P42, were stained with Iba1 and CD68 to more broadly mark actively phagocytosing cells. Iba1 positive microglial cells were clearly observed in the IPL, OPL, ONL and SRS, in vehicle injected mice, but the number of Iba1 positive cells in the ONL and SRS was significantly reduced in mice treated with minocycline at both 3 weeks (**Fig.s 6A & 6C**) and 6 weeks (**Fig.s 6B & 6D**) of age, with the majority of microglia residing in the IPL and OPL. Furthermore, co-localization of CD68 and Iba1 was evident in the OPL, ONL and SRS in vehicle injected mice, but this was greatly reduced in minocycline-injected animals. As the majority of cells that were CD68+Iba1+ double-positive were those that had migrated towards the dying photoreceptors, it was difficult to decipher whether minocycline was simply slowing down the migration of these cells towards the SRS or whether minocycline was directly reducing the cells' phagocytic ability. To overcome this we examined whether minocycline could alter the phagocytic capacity of microglia in a basal state *in vitro*. Untreated and minocycline-treated BV2 cells were incubated with green fluorescent latex beads for 3 hours and internalization of the beads was measured by immunofluorescence (**Fig. 6E**). Indeed, minocycline treatment resulted

in a marked reduction in the number of BV2 cells that had engulfed the latex beads compared to untreated cells (**Fig. 6F),** indicating that minocycline could directly reduce the basal phagocytic capacity of these cells.

Finally, we assessed the therapeutic efficacy of minocycline administration in our *Rho-/-*model. As before, minocycline was administered by two daily injections from P16 to P42 and we evaluated retinal degeneration *in vivo* by optical coherence tomography (OCT). OCT uses infra-red light waves to take cross section images of the retina and is a non-invasive mode of measuring retinal thickness and *abnormalities in vivo*. We measured the distance between the OPL (which forms the interface between the bipolar cells and photoreceptors) and the RPE to get the thickness of both the ONL and the photoreceptor segments and found a substantial preservation in retinal thickness in minocycline-injected *Rho-/-*mice (**Fig. 6G**). We also examined photoreceptor cell death by H&E staining of paraffin-embedded retinal tissue sections from these mice. We counted the number of nuclei rows in the ONL of each eye at 12 points along the vertical meridian from sections cut on a sagittal plane through the optic nerve head at ~150 and ~250 μm from the periphery (**Fig. 6I**). In support of the OCT data depicting minocycline-induced preservation of retinal thickness, ONL counts indicated minocycline attenuated photoreceptor cell death in the *Rho-/-*mice with a significant preservation of the numbers of photoreceptor rows still remaining at 6 weeks of age (**Fig. 6J**). Quantification of the distance from the RPE to the external limiting membrane demonstrated no significant changes with minocycline treatment, indicating that minocycline preserves photoreceptor cell numbers and not the length of the inner segments of the rods, and inner and outer segments of the cones (**Fig. 6I**).

Discussion

As the resident immune cells in the retina, microglia play important homeostatic roles in retinal immune regulation and neuroprotection. However, under continuous pathological insult, uncontrolled and chronic microglia activation ensues, and is a common hallmark of many degenerative retinal diseases. Here, we investigate how minocycline, a semi-synthetic tetracycline analogue, affects molecular signatures of homeostatic and disease-associated microglia (DAM) *in vivo* using the *Rho-/-*model of retinal degeneration and *in vitro* using the murine microglia BV2 cell line. Due to the recent surge in single cell RNA transcriptomics, microglia signatures in homeostatic versus diseased phenotypes have been well defined, identifying this DAM subtype. The activation of homeostatic microglia into DAM is a two-step process, with a clear intermediary state observed. In the initial stage, there is a downregulation of microglial homeostatic genes (*e.g. P2ry12, Cx3cr1, Tmem119, Tgfbr1*) along with the upregulation of a subset of DAM genes (*e.g. Tryobp, Apoe, B2m and Ctsb*). Induction of the key genes involved in lipid metabolism and phagocytosis (*e.g. Lpl, Itgax, Clec7a, Trem2*) are not observed until the second stage of DAM activation, a stage which is dependent on TREM2 signalling (Keren-Shaul, Spinrad et al. 2017).

Here, we found that microglia are activated and infiltrate the outer retina in the *Rho-/-* model, and this is observed from even 3 weeks of age at the onset of photoreceptor cell death. These microglia infiltrating the SRS are actively phagocytosing and express the DAM marker LPL. Surprisingly, LPL appears only to be induced on encountering the lipid rich environment in the inner and outer segments. Even on traversing through the ONL, we observe no LPL positive stain on the inner retinal side of the external limiting membrane (ELM), despite these microglia being positive for the phagocytic marker CD68; CD68 is apparent in $Iba1^{+}$ and $P2RY12^{+}$ cells in

393 the INL prior to deeper infiltration into the outer retina. Of note, LPL has been shown to co-
394 localize with microglia that have internalized amyloid beta (Aβ) in mouse and human brains
395 (Keren-Shaul, Spinrad et al. 2017), suggesting that LPL plays a direct role in Aβ uptake and
396 perhaps, in our *Rho-/-*model, only the microglia that have already phagocytosed the
397 photoreceptor segments in the SRS are LPL positive.

398 Minocycline has been widely used in CNS studies as a microglial inhibitor, however, its
399 effect on the DAM profile has never been investigated. Thus, we next explored whether
400 minocycline could modify DAM signature genes in the retina of *Rho-/-*mice as well as in BV2
401 microglial cells directly. Interestingly, we found that *Sall1* levels showed a decrease with
402 minocycline treatment in *Rho-/-*animals while the remainder of the homeostatic genes, *P2ry12,*
403 *Cx3cr1, Tmem119, Tgfbr1* and *Selplg* remained unchanged. *Sall1* encodes a transcription
404 regulator that dampens a reactive microglia phenotype allowing them to conduct their
405 physiological functions (Buttgereit, Lelios et al. 2016), so it is surprising that this gene was
406 down-regulated with minocycline. However, minocycline did not directly alter this or any other
407 homeostatic genes in microglia *in vitro*.

408 Remarkably, many genes associated with both the first (*Tyrobp*, *Apoe* and *Ctsb*) and
409 second stage (*Lpl, Csf1r and Clec7a*) of DAM activation were down-regulated with minocycline
410 treatment in the retinas from *Rho-/-*animals and/or BV2 microglia. TYROBP is a cytoplasmic
411 adaptor protein for the immunoreceptor TREM2, and this signalling complex promotes Aβ
412 clearance, enhancing microglial phagocytosis while supressing inflammatory cytokine
413 production and secretion from these cells (Ma, Jiang et al. 2015). Furthermore, triggering of this
414 receptor induces APOE activation, and the APOE-TREM2 signalling pathway has been shown to
415 be a critical regulator of microglia phenotypic change in neurodegenerative disease (Krasemann,

Madore et al. 2017). Intriguingly, a recent study has reported possible APOE-TYROBP signalling independent of TREM2 and propose that this pathway could be an early or initiating step in DAM activation (Audrain, Haure-Mirande et al. 2021). Although, *Trem2* levels remained unchanged, both *Apoe* and *Tyrobp* levels decreased with minocycline treatment, suggesting that minocycline could reduce TYROBP levels, leading to decreased TREM2 activation and in turn reduced APOE-TREM2 signalling, halting DAM phenotype activation. Additionally, minocycline could also reduce this recently reported APOE-TYROBP signalling directly, dampening the initiation of DAM.

Upregulation of phagocytic and lipid metabolism genes are characteristic of stage two DAM activation suggesting a preference of lipids to fuel the greater bioenergetics needs of these phagocytic microglia (Loving and Bruce 2020). Indeed, knockdown of LPL in BV2 cells has previously been shown to reduce microglial phagocytosis of Aβ (Ma, Bao et al. 2013). Here, we found that minocycline reduced LPL levels in *Rho-/-*retina and in BV2 microglia both at the transcriptional and protein level. *Clec7a*, the gene encoding the pattern recognition receptor, Dectin-1, is a known inducer of LC3-associated phagocytosis (Ma, Becker et al. 2012) and although expressed at very low levels in the *Rho-/-*retina and BV2 microglia, minocycline also significantly reduced *Clec7a* expression.

Lgals3, the gene encoding Galectin-3, and *Itgax* (Integrin subunit alpha X), encoding CD11c were two DAM genes surprisingly increased with minocycline in the *Rho-/-*retinas. Galectin-3 has been found to be highly upregulated in the brains of neurodegenerative disease and was recently identified as a novel endogenous TREM2 ligand (Boza-Serrano, Ruiz et al. 2019). Although an increase in *Lgals3* was observed transcriptionally in *Rho-/-*retinas, this galectin is also expressed in other retinal cells such as Muller glia, and indeed, minocycline

failed to alter both *Lgals3* transcriptional and Galectin-3 protein levels in the BV2 microglia cells. Similarly, *Itgax* which is also expressed in vascular endothelial cells and Muller glia, remained unchanged in minocycline-treated BV2 cells.

As many of the DAM genes minocycline targeted were involved in phagocytosis, we examined the basal phagocytic capacity of microglia *in vitro* and found that minocycline directly reduced microglial phagocytosis in these cells. Furthermore, we discovered that these minocycline treated microglia, which had a reduced phagocytic capacity and DAM phenotype, could attenuate photoreceptor cell loss in the *Rho-/-*model of retinal degeneration. *Rho-/-*mice that were administered with minocycline from P16-42, had delayed retinal thinning than vehicle injected mice when examined *in vivo* by OCT imaging and from analysis of H&E stained retinal sections.

Overall, our data supports other studies demonstrating the therapeutic efficacy of minocycline in retinal degeneration; minocycline treatment has previously been shown to preserve the morphology and function of photoreceptors in the *rd10* mouse model (Peng, Xiao et al. 2014), in a light-damage-induced RD model (Scholz, Sobotka et al. 2015) and more recently, in the *Mertk*$^{-/-}$ mouse model of RD (Terauchi, Kohno et al. 2021). It is important to consider, however, that triggering early DAM activation may be useful to induce a microglia response in diseases where a strong phagocytic activity might be beneficial. Indeed, a recent study using single-cell RNA sequencing to characterize the transcriptome of sub-retinal microglia (srMG) in a light damage model of photoreceptor degeneration as well as a genetic model (Rho$^{P23H/WT}$) of chronic retinal degeneration (O'Koren, Yu et al. 2019) found that the srMG expressing many DAM markers protected the RPE from disease-associated damage in both models. Additionally, in a model of acute retinal detachment, microglia have been shown to be protective, by rapidly

462 phagocytosing damaging cell debris to avoid triggering apoptosis of neighbouring photoreceptors
463 and also by its close association and control of macrophage infiltration (Okunuki, Mukai et al.
464 2018). However, their appearance in our *Rho-/-*model indicate that these mechanisms may be
465 disadvantageous under different conditions. Activation of LPL on reaching the SRS may give
466 microglia an enhanced phagocytic capacity which may cause premature phagocytosis of
467 otherwise functional photoreceptor cells/segments. Phagocytosis of damaged and dying
468 photoreceptors is important to protect neighbouring healthy cells but overt phagocytosis may
469 enable retinal degeneration to advance at a more progressive rate than otherwise possible.
470 As microglia participate in vital physiological functions in the retina, complete
471 obliteration or blocking of all retinal microglial functions is undesirable (Wang, Zhao et al.
472 2016). Therefore, immunotherapeutic approaches that focus on targeting specific aspects of the
473 microglial phagocytic pathway, e.g. LPL, TYROBP, may be of benefit. Alternatively, targeting
474 the lipid catabolism pathway directly may provide another therapeutic avenue. Furthermore,
475 dampening these over-reactive microglia with minocycline in combination with drugs that target
476 photoreceptor cell death, or promote cell survival pathways, may present a broadly applicable
477 therapy more readily accessible for people with inherited retinopathies.
478
479 **Conclusions:** Overall, our study provides compelling evidence that targeting excessive microglia
480 phagocytosis may be a druggable intervention for some retinal degenerative diseases, and
481 identifies microglial lipid processing enzyme and DAM-marker LPL as a direct target of
482 minocycline indicating that suppression of lipid metabolism is one mechanism by which
483 minocycline protects against inflammation induced photoreceptor cell death.
484

Figure Legends

Figure 1: Microglia are activated and infiltrate the outer retina over time in the rhodopsin knockout (*rho*$^{-/-}$) model of photoreceptor degeneration.

(**A**) Retinal flatmounts from WT and *Rho-/-*mice at 3, 6, 9 and 12 weeks of age stained with the microglia marker Iba1 (20X magnification) with (**a'-h'**) magnified and skeleton images. (**B**) Retinal cryosections from WT and *Rho-/-*mice at 3, 6, 9 and 12 weeks of age stained with the microglia marker Iba1 (40X magnification, nuclei staining - Hoechst), with (**a'-h'**) magnified images of the ONL and sub-retinal space shown to the right. (IPL – inner plexiform layer, INL – inner nuclear layer, ONL outer nuclear layer).

Figure 2: Microglia infiltrating the sub-retinal space are actively phagocytosing photoreceptor cells

(**A**) Retinal cryosections from WT mice and *Rho-/-*mice at 3, 6, 9 and 12 weeks of age stained with Iba1 and CD68 (40X magnification) with magnified images of *Rho-/-*mice at (**a'**) 3 and (**b'**) 6 weeks. (**B**) Retinal cryosections from WT mice and *Rho-/-*mice at 3, 6, 9 and 12 weeks of age stained with P2RY12 and CD68 (40X magnification) with magnified images of *Rho-/-*mice at (**a'**) 3 and (**b'**) 6 weeks (nuclei staining - Hoechst, arrows indicate areas of co-staining). (IPL – inner plexiform layer, INL – inner nuclear layer, ONL outer nuclear layer, LPL – lipoprotein lipase).

Figure 3: Microglia infiltrating the sub-retinal space express disease-associated microglia (DAM) marker LPL.

(**A**) Retinal cryosections from WT mice and *Rho-/-*mice at 3, 6, 9 and 12 weeks of age stained with Iba1 and LPL (40X magnification) with magnified images of *Rho-/-*mice at (**a'**) 3, (**b'**) 6, (**c'**) 9 and (**d'**) 12 weeks (nuclei staining - Hoechst, arrows indicate areas of co-staining). (IPL – inner plexiform layer, INL – inner nuclear layer, ONL outer nuclear layer, LPL – lipoprotein lipase).

Figure 4: Minocycline regulates microglia activation, downregulating DAM genes in the rhodopsin knockout (*rho*$^{-/-}$) model of retinal degeneration.

(**A**) Iba1-stained retinal flatmounts from *Rho-/-*mice at 3 weeks of age given intra-peritoneal injections of vehicle or minocycline (50 mg/kg) twice daily from post-natal day 16 (P16) to P21 with (**B**) microglial activation quantified by area grid analysis. (**C**) RT-PCR analysis of homeostatic and DAM gene transcript levels in the neural retina from these minocycline- or vehicle-injected *Rho-/-*mice at 3 weeks of age with a (**D**) heatmap showing the level of expression normalized to the housekeeping gene ubiquitin C (*$P \leq 0.05$, **$P \leq 0.01$, ***$P \leq 0.001$ by *t* test, n = 5-6 mice). (**E**) Retinal cryosections from these minocycline- or vehicle-injected *Rho-/-*mice at 3 weeks of age stained with Iba1 and the DAM gene LPL. (IPL – inner plexiform layer, INL – inner nuclear layer, ONL outer nuclear layer, LPL – lipoprotein lipase).

Figure 5: Minocycline directly regulates DAM gene expression in BV2 microglia in vitro.

(**A**) RT-PCR analysis of homeostatic and DAM gene transcript levels in BV2 microglial cells that were untreated or treated with 5 ug/ml Minocycline for 7 h with a (**B**) heatmap showing the level of expression normalized to the housekeeping gene ubiquitin C (***$P \leq 0.001$ by *t* test, n = 3 biological replicates). (**C, D, E, F**) Western blot analysis of LPL, APOE, CSF1R and Galectin-

3 expression levels in BV2 microglial cells that were untreated or treated with 5 ug/ml minocycline for 24 h with densitometry shown to the right (**$P \leq 0.01$, ***$P \leq 0.001$ by *t* test, *n* = 3 biological replicates).

Figure 6: Minocycline inhibits microglial phagocytic function and supports photoreceptor survival in the rhodopsin knockout (*rho*$^{-/-}$) model of retinal degeneration.

(**A, B, C, D**) Iba1- and CD68-stained retinal cryosections from *Rho-/-*mice at 3 weeks and 6 weeks of age given intra-peritoneal injections of vehicle or minocycline (50 mg/kg) twice daily from post-natal day 16 (P16) to P21 or from P16 to P42 with microglial activation quantified by area grid analysis. (**E**) Immunocytochemistry of BV2 microglial cells that were untreated or treated with 5 ug/ml minocycline for 24 h and exposed to fluorescent opsonized latex beads for 3h before fixation and stained with MitoTracker and Hoechst. (**F**) Quantification of BV2 phagocytic activity expressed as percentage of bead^{+} cells (***$P \leq 0.001$ by *t* test, data representative of 3 separate experiments with 3 fields of view imaged per well). (**G, H**) Optical coherence tomography (OCT) images taken *in vivo* from from *Rho-/-*mice at 6 weeks of age given intra-peritoneal injections of vehicle or minocycline (50 mg/kg) twice daily from post-natal P16 to P42 with quantification of the ONL to the outer segment (OS) width (marked with red line in the OCT images) using *ImageJ* (*$P \leq 0.05$, $n = 3–6$ mice per group). (**I, J, K**) Haemotoxylin and eosin staining of paraffin-embedded sections from these minocycline- or vehicle-treated *Rho-/-*mice at 6 weeks with quantification of the number of photoreceptor rows in the ONL and quantification of the inner and outer segment length using *ImageJ* (*$P \leq 0.05$, *n* = 3–6 mice per group). (GCL – ganglion cell layer, INL – inner nuclear layer, ONL outer nuclear layer).

Abbreviations:

Apolipoprotein E (APOE)

central nervous system (CNS)

colony stimulating factor 1 (CSF1R)

disease associated microglia (DAM)

external limiting membrane (ELM)

Haemotoxylin and Eosin (H&E)

inner plexiform (IPL)

Ionized calcium binding adaptor molecule 1 (Iba1)

Leber congenital amaurosis (LCA)

lipoprotein lipase (LPL)

Optical coherence tomography (OCT)

outer nuclear layer (ONL)

outer plexiform layers (OPL)

Phosphate buffer saline (PBS)

Retinitis pigmentosa (RP)

rhodopsin knockout mice (*rho*$^{-/-}$)

Ribonucleic acid (RNA)

sub-retinal space (SRS)

Transmembrane Immune Signaling Adaptor (TYROBP)

Triggering Receptor Expressed On Myeloid Cells 2 (TREM2)

Purinergic Receptor P2Y12 (P2ry12)

Declarations

Ethical approval: All animal studies carried out in the Smurfit Institute of Genetics in TCD adhere to the principles laid out by the internal ethics committee at TCD, and all relevant national licenses were obtained before commencement of all studies.

Consent for publication: Not applicable.

Availability of data and materials: Data sharing not applicable to theis article a no datasets were generated during this current study.

Competing Interests: The authors declare that they have no competing interests

Funding: SFI-15 CDA/3497, SFI-18/TIDA/6067, IRCLA/2017/295,
HRB/MRCG-2018-08, NCRC/18/10, ERC (Retina Rhythm – 864522).

Authors contributions: EO and CD performed experiments and analysed data, SD directed the research. EO, MC and SD wrote the manuscript. All authors read and approved the final manuscript

Acknowledgements: Not applicable

References

Audrain, M., J. V. Haure-Mirande, J. Mleczko, M. Wang, J. K. Griffin, P. H. St George-Hyslop, P. Fraser, B. Zhang, S. Gandy and M. E. Ehrlich (2021). "Reactive or transgenic increase in microglial TYROBP reveals a TREM2-independent TYROBP-APOE link in wild-type and Alzheimer's-related mice." Alzheimers Dement **17**(2): 149-163.

Dannhausen, K., C. Möhle and T. Langmann (2018). "Immunomodulation with minocycline rescues retinal degeneration in juvenile neuronal ceroid lipofuscinosis mice highly susceptible to light damage." Dis Model Mech **11**(9).

Humphries, M. M., D. Rancourt, G. J. Farrar, P. Kenna, M. Hazel, R. A. Bush, P. A. Sieving, D. M. Sheils, N. McNally, P. Creighton, A. Erven, A. Boros, K. Gulya, M. R. Capecchi and P. Humphries (1997). "Retinopathy induced in mice by targeted disruption of the rhodopsin gene." Nat Genet **15**(2): 216-219.

Karperien, A., H. Ahammer and H. F. Jelinek (2013). "Quantitating the subtleties of microglial morphology with fractal analysis." Front Cell Neurosci **7**: 3.

Keren-Shaul, H., A. Spinrad, A. Weiner, O. Matcovitch-Natan, R. Dvir-Szternfeld, T. K. Ulland, E. David, K. Baruch, D. Lara-Astaiso, B. Toth, S. Itzkovitz, M. Colonna, M. Schwartz and I. Amit (2017). "A Unique Microglia Type Associated with Restricting Development of Alzheimer's Disease." Cell **169**(7): 1276-1290.e1217.

Kobayashi, K., S. Imagama, T. Ohgomori, K. Hirano, K. Uchimura, K. Sakamoto, A. Hirakawa, H. Takeuchi, A. Suzumura, N. Ishiguro and K. Kadomatsu (2013). "Minocycline selectively inhibits M1 polarization of microglia." Cell Death Dis **4**(3): e525.

614 Kohno, H., Y. Chen, B. M. Kevany, E. Pearlman, M. Miyagi, T. Maeda, K. Palczewski and A.
615 Maeda (2013). "Photoreceptor proteins initiate microglial activation via Toll-like receptor 4 in
616 retinal degeneration mediated by all-trans-retinal." J Biol Chem **288**(21): 15326-15341.
617 Krasemann, S., C. Madore, R. Cialic, C. Baufeld, N. Calcagno, R. El Fatimy, L. Beckers, E.
618 O'Loughlin, Y. Xu, Z. Fanek, D. J. Greco, S. T. Smith, G. Tweet, Z. Humulock, T. Zrzavy, P.
619 Conde-Sanroman, M. Gacias, Z. Weng, H. Chen, E. Tjon, F. Mazaheri, K. Hartmann, A. Madi, J.
620 D. Ulrich, M. Glatzel, A. Worthmann, J. Heeren, B. Budnik, C. Lemere, T. Ikezu, F. L. Heppner,
621 V. Litvak, D. M. Holtzman, H. Lassmann, H. L. Weiner, J. Ochando, C. Haass and O. Butovsky
622 (2017). "The TREM2-APOE Pathway Drives the Transcriptional Phenotype of Dysfunctional
623 Microglia in Neurodegenerative Diseases." Immunity **47**(3): 566-581.e569.
624 Loving, B. A. and K. D. Bruce (2020). "Lipid and Lipoprotein Metabolism in Microglia." Front
625 Physiol **11**: 393.
626 Ma, J., C. Becker, C. A. Lowell and D. M. Underhill (2012). "Dectin-1-triggered recruitment of
627 light chain 3 protein to phagosomes facilitates major histocompatibility complex class II
628 presentation of fungal-derived antigens." J Biol Chem **287**(41): 34149-34156.
629 Ma, J., T. Jiang, L. Tan and J. T. Yu (2015). "TYROBP in Alzheimer's disease." Mol Neurobiol
630 **51**(2): 820-826.
631 Ma, Y., J. Bao, X. Zhao, H. Shen, J. Lv, S. Ma, X. Zhang, Z. Li, S. Wang, Q. Wang and J. Ji
632 (2013). "Activated cyclin-dependent kinase 5 promotes microglial phagocytosis of fibrillar β-
633 amyloid by up-regulating lipoprotein lipase expression." Mol Cell Proteomics **12**(10): 2833-
634 2844.
635 Murakami, Y., K. Ishikawa, S. Nakao and K. H. Sonoda (2020). "Innate immune response in
636 retinal homeostasis and inflammatory disorders." Prog Retin Eye Res **74**: 100778.

637 O'Koren, E. G., C. Yu, M. Klingeborn, A. Y. W. Wong, C. L. Prigge, R. Mathew, J. Kalnitsky,
638 R. A. Msallam, A. Silvin, J. N. Kay, C. Bowes Rickman, V. Y. Arshavsky, F. Ginhoux, M.
639 Merad and D. R. Saban (2019). "Microglial Function Is Distinct in Different Anatomical
640 Locations during Retinal Homeostasis and Degeneration." Immunity **50**(3): 723-737.e727.
641 Okunuki, Y., R. Mukai, E. A. Pearsall, G. Klokman, D. Husain, D. H. Park, E. Korobkina, H. L.
642 Weiner, O. Butovsky, B. R. Ksander, J. W. Miller and K. M. Connor (2018). "Microglia inhibit
643 photoreceptor cell death and regulate immune cell infiltration in response to retinal detachment."
644 Proc Natl Acad Sci U S A **115**(27): E6264-e6273.
645 Ozaki, E., L. Gibbons, N. G. Neto, P. Kenna, M. Carty, M. Humphries, P. Humphries, M.
646 Campbell, M. Monaghan, A. Bowie and S. L. Doyle (2020). "SARM1 deficiency promotes rod
647 and cone photoreceptor cell survival in a model of retinal degeneration." Life Sci Alliance **3**(5).
648 Peng, B., J. Xiao, K. Wang, K. F. So, G. L. Tipoe and B. Lin (2014). "Suppression of microglial
649 activation is neuroprotective in a mouse model of human retinitis pigmentosa." J Neurosci
650 **34**(24): 8139-8150.
651 Scholz, R., M. Sobotka, A. Caramoy, T. Stempfl, C. Moehle and T. Langmann (2015).
652 "Minocycline counter-regulates pro-inflammatory microglia responses in the retina and protects
653 from degeneration." J Neuroinflammation **12**: 209.
654 Terauchi, R., H. Kohno, S. Watanabe, S. Saito, A. Watanabe and T. Nakano (2021).
655 "Minocycline decreases CCR2-positive monocytes in the retina and ameliorates photoreceptor
656 degeneration in a mouse model of retinitis pigmentosa." PLoS One **16**(4): e0239108.
657 Wang, X., L. Zhao, J. Zhang, R. N. Fariss, W. Ma, F. Kretschmer, M. Wang, H. H. Qian, T. C.
658 Badea, J. S. Diamond, W. B. Gan, J. E. Roger and W. T. Wong (2016). "Requirement for

659 Microglia for the Maintenance of Synaptic Function and Integrity in the Mature Retina." J
660 Neurosci **36**(9): 2827-2842.
661 Zhang, C., B. Lei, T. T. Lam, F. Yang, D. Sinha and M. O. Tso (2004). "Neuroprotection of
662 photoreceptors by minocycline in light-induced retinal degeneration." Invest Ophthalmol Vis Sci
663 **45**(8): 2753-2759.
664

Figure 1

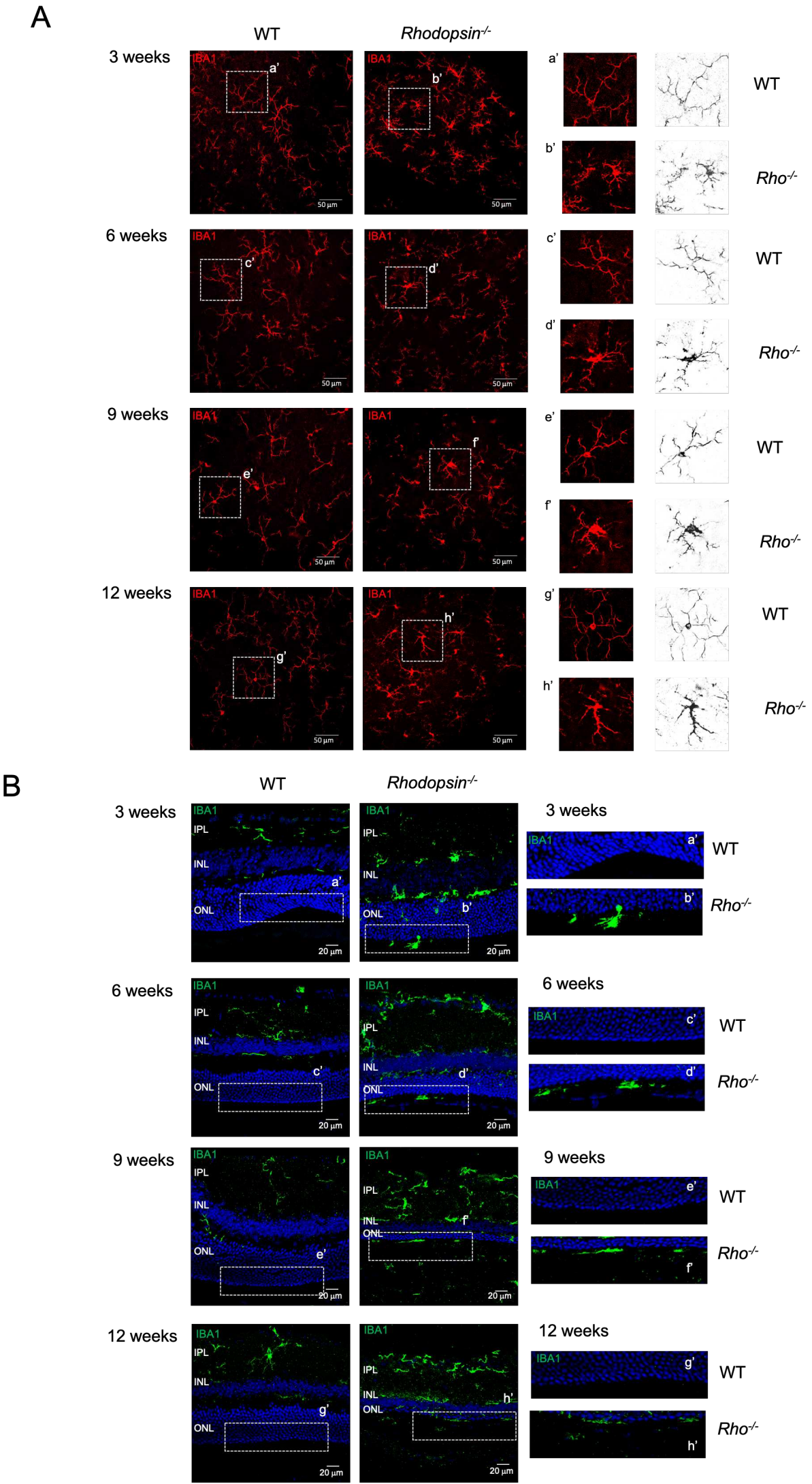
A
WT
Rhodopsin-/-
3 weeks
6 weeks
9 weeks
12 weeks
IBA1
a'
b'
c'
d'
e'
f'
g'
h'
50 µm
WT
Rho-/-
B
IPL
INL
ONL
20 µm

Figure 2

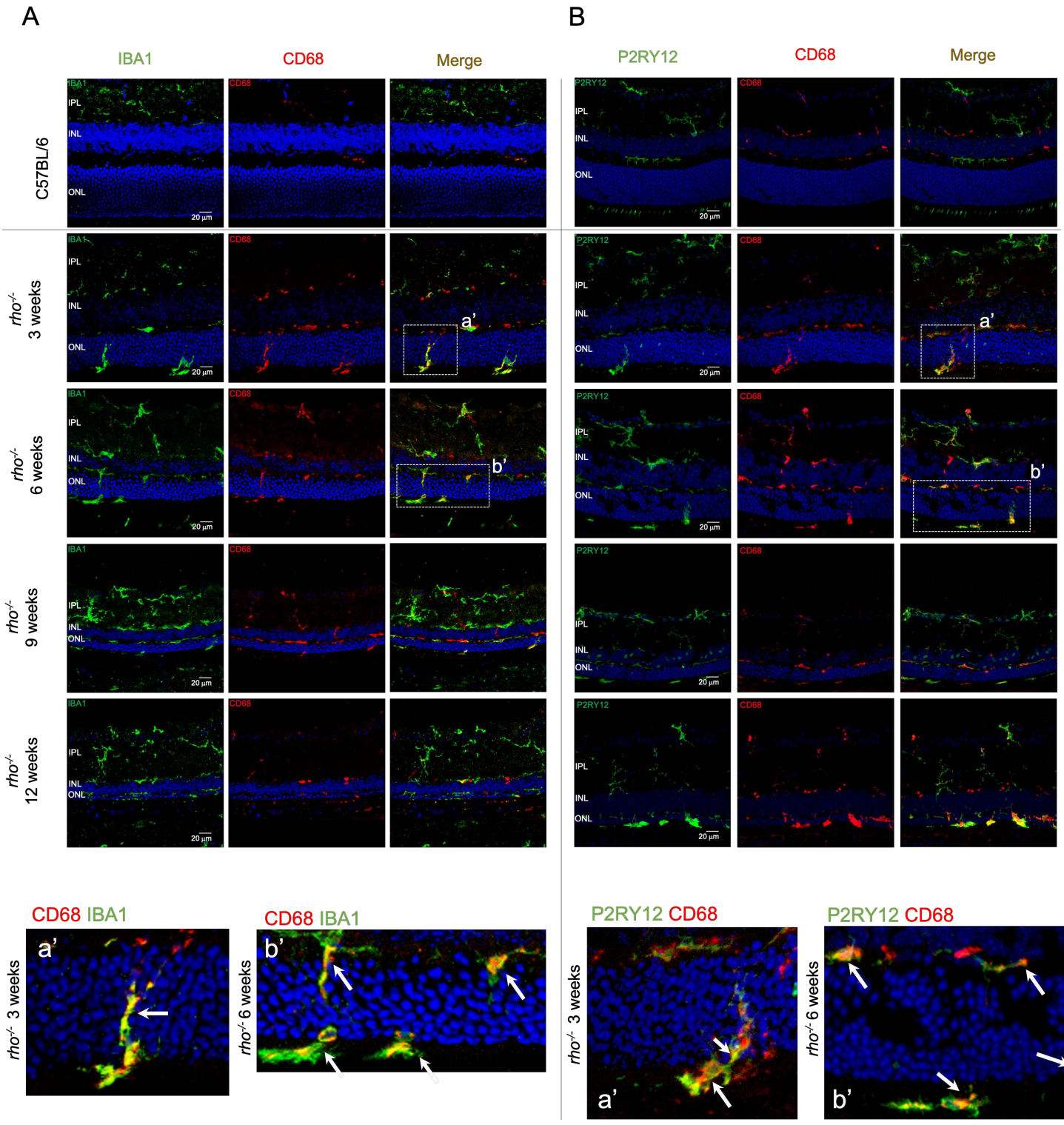
A
B
IBA1
CD68
Merge
P2RY12
C57BL/6
rho-/- 3 weeks
rho-/- 6 weeks
rho-/- 9 weeks
rho-/- 12 weeks
IPL
INL
ONL
20 µm
a'
b'
CD68 IBA1
P2RY12 CD68
rho-/- 3 weeks
rho-/- 6 weeks

Figure 3

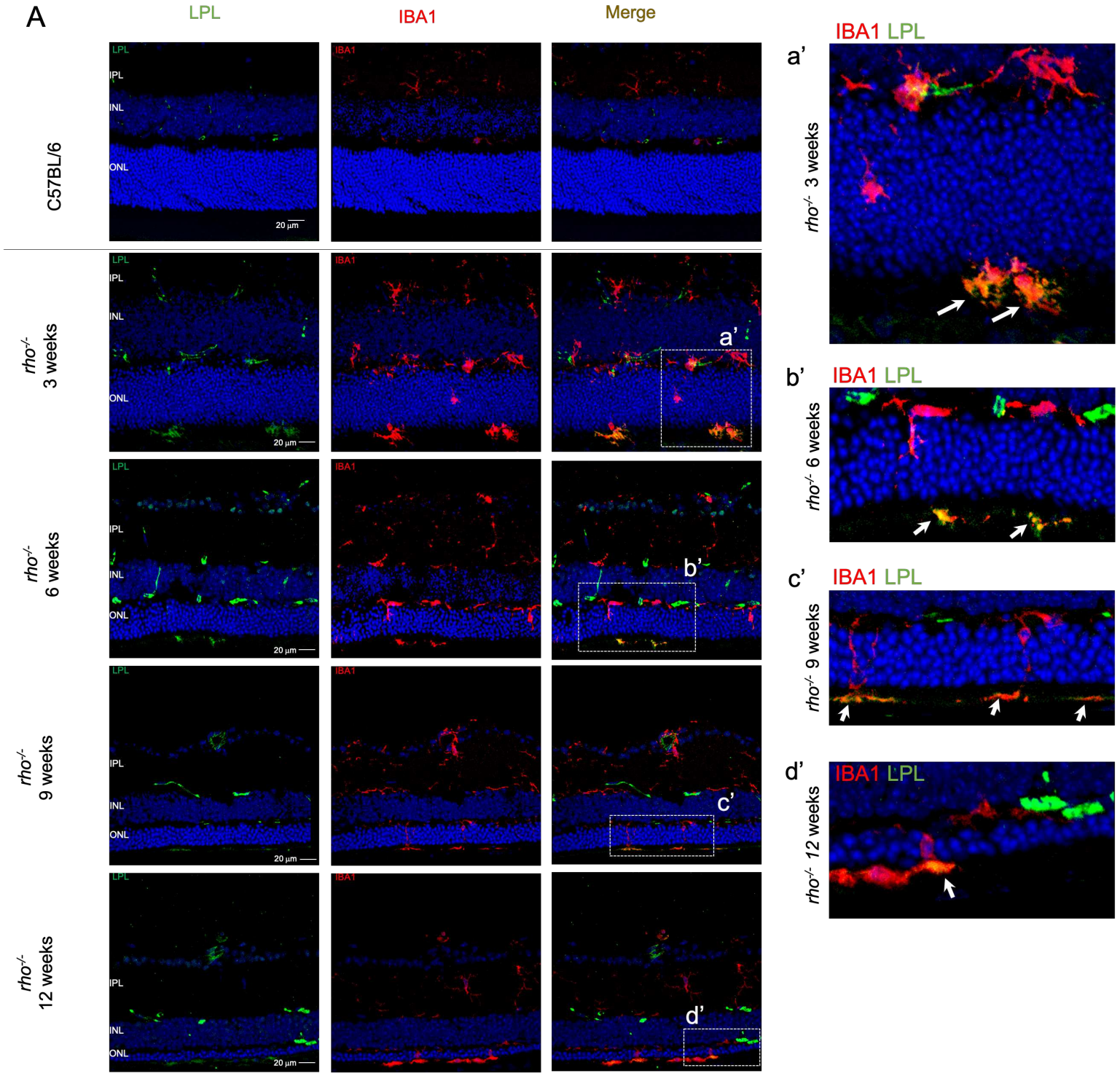
A
LPL
IBA1
Merge
C57BL/6
rho-/- 3 weeks
rho-/- 6 weeks
rho-/- 9 weeks
rho-/- 12 weeks
IPL
INL
ONL
20 µm
a'
b'
c'
d'
IBA1 LPL
rho-/- 3 weeks
rho-/- 6 weeks
rho-/- 9 weeks
rho-/- 12 weeks

Figure 4

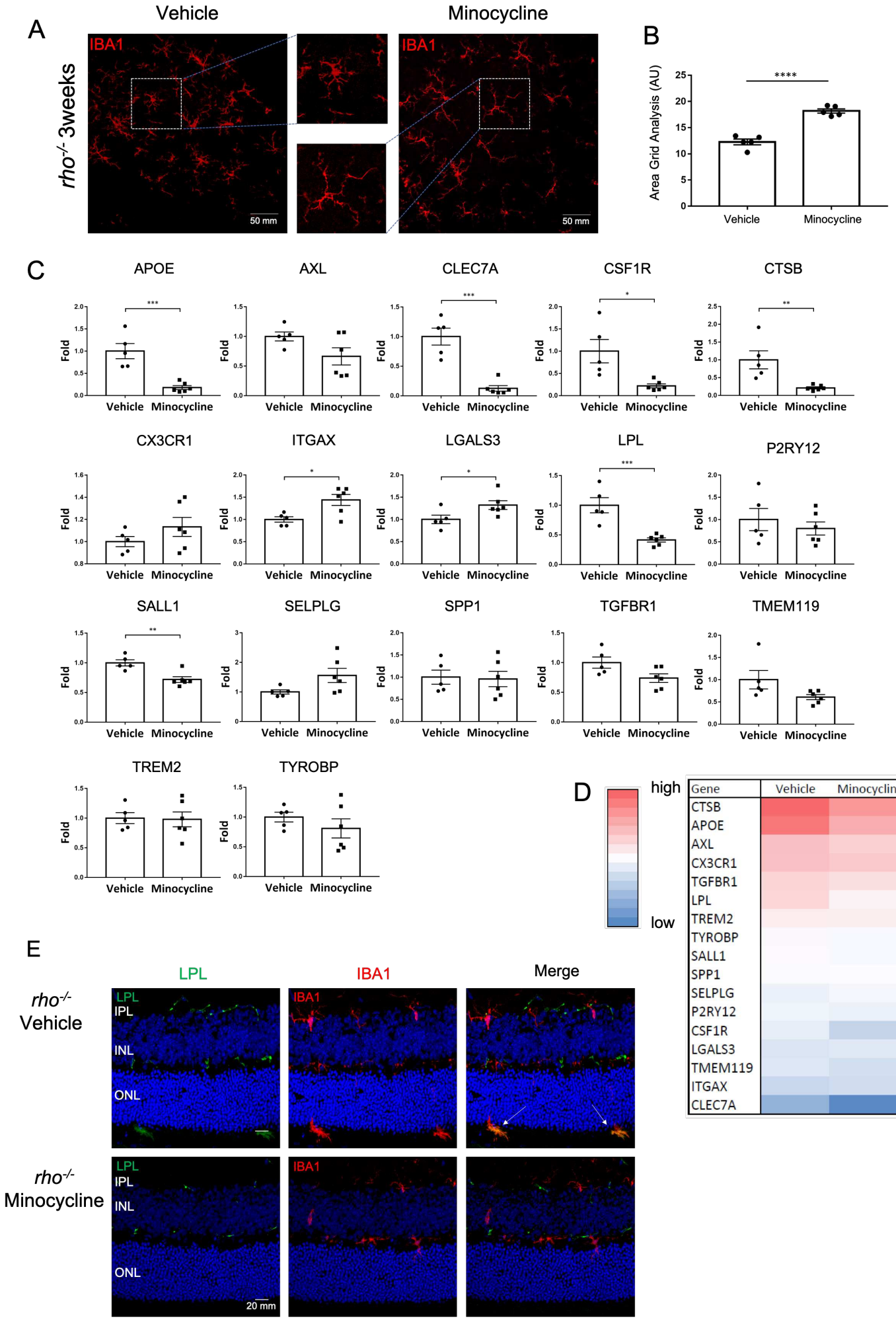
A
Vehicle
Minocycline
rho-/- 3weeks
IBA1
IBA1
50 mm
50 mm
B
Area Grid Analysis (AU)
****
Vehicle
Minocycline
C
APOE
AXL
CLEC7A
CSF1R
CTSB
CX3CR1
ITGAX
LGALS3
LPL
P2RY12
SALL1
SELPLG
SPP1
TGFBR1
TMEM119
TREM2
TYROBP
Fold
Vehicle
Minocycline
D
high
low
Gene
Vehicle
Minocycline
CTSB
APOE
AXL
CX3CR1
TGFBR1
LPL
TREM2
TYROBP
SALL1
SPP1
SELPLG
P2RY12
CSF1R
LGALS3
TMEM119
ITGAX
CLEC7A
E
LPL
IBA1
Merge
rho-/-
Vehicle
rho-/-
Minocycline
LPL
IPL
INL
ONL
IBA1
20 mm

Figure 5

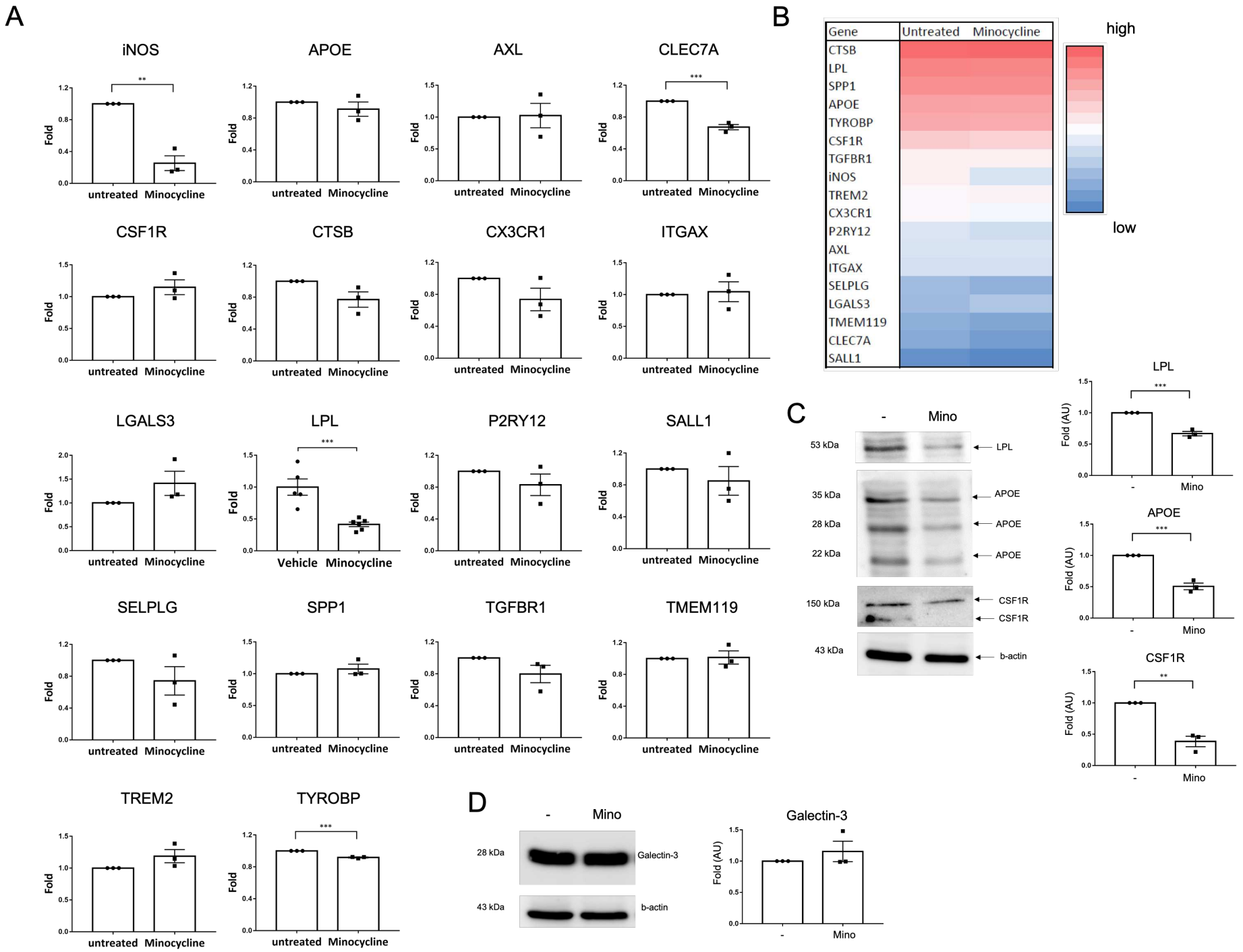
A
iNOS
APOE
AXL
CLEC7A
CSF1R
CTSB
CX3CR1
ITGAX
LGALS3
LPL
P2RY12
SALL1
SELPLG
SPP1
TGFBR1
TMEM119
TREM2
TYROBP
Fold
untreated
Minocycline
Vehicle
B
Gene
Untreated
Minocycline
high
low
C
-
Mino
53 kDa
35 kDa
28 kDa
22 kDa
150 kDa
43 kDa
LPL
APOE
CSF1R
b-actin
Fold (AU)
D
28 kDa
Galectin-3
43 kDa
b-actin

Figure 6

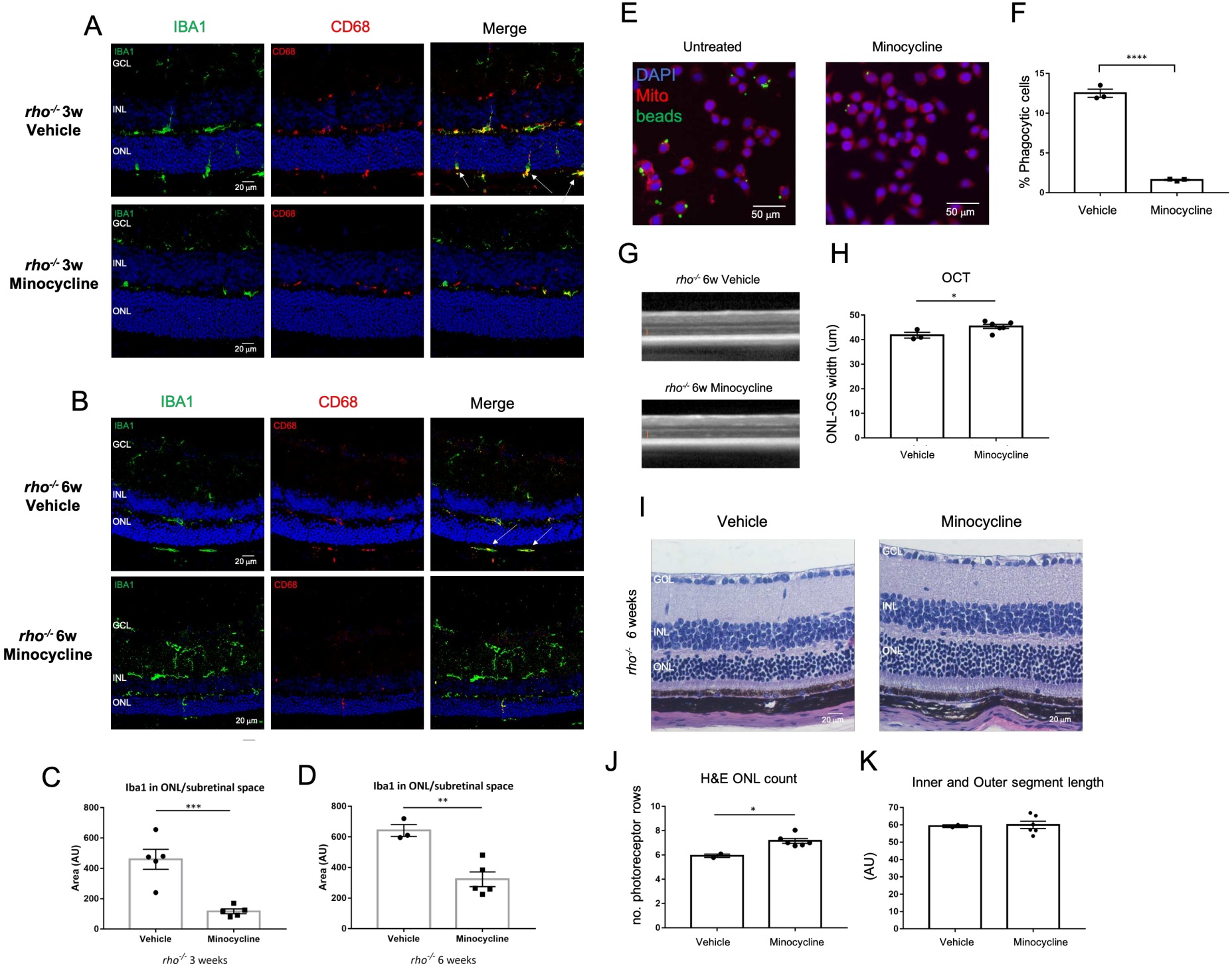
A
IBA1
CD68
Merge
rho-/- 3w Vehicle
rho-/- 3w Minocycline
GCL
INL
ONL
20 µm
B
rho-/- 6w Vehicle
rho-/- 6w Minocycline
C
Iba1 in ONL/subretinal space
Area (AU)
Vehicle
Minocycline
rho-/- 3 weeks
D
rho-/- 6 weeks
E
Untreated
Minocycline
DAPI
Mito
beads
50 µm
F
% Phagocytic cells
****
G
rho-/- 6w Vehicle
rho-/- 6w Minocycline
H
OCT
ONL-OS width (um)
I
rho-/- 6 weeks
GCL
INL
ONL
J
H&E ONL count
no. photoreceptor rows
K
Inner and Outer segment length
(AU)